Circulating circRNA as Biomarkers For Dilated Cardiomyopathy Etiology

Marina Costa*
Instituto de Medicina Molecular: Universidade de Lisboa Instituto de Medicina Molecular Joao Lobo Antunes
Maria Calderon-Dominguez* (mariacalderond@gmail.com)
Biomedical Research Institute of Cadiz https://orcid.org/0000-0003-1797-3450
Alipio Mangas
University of Cadiz Faculty of Medicine: Universidad de Cadiz Facultad de Medicina
Oscar Campuzano
University of Girona Faculty of Medicine: Universitat de Girona Facultat de Medicina
Georgia Sarquella-Brugada
University of Girona Faculty of Medicine: Universitat de Girona Facultat de Medicina
Monica Ramos
Universidad Alfonso X El Sabio
Maribel Quezada-Feijoo
Universidad Alfonso X El Sabio
José Manuel García Pinilla
Hospital Universitario Virgen de la Victoria
Ainhoa Robles-Mezcua
Hospital Universitario Virgen de la Victoria
Thalia Belmonte
Biomedical Research Institute of Cadiz
Francisco J Enguita
Instituto de Medicina Molecular: Universidade de Lisboa Instituto de Medicina Molecular Joao Lobo Antunes
Rocio Toro
University of Cadiz Faculty of Medicine: Universidad de Cadiz Facultad de Medicina

Research Article

Keywords: Circulating circular RNA, ischemic-dilated cardiomyopathy, Lamin A/C-dilated cardiomyopathy

Posted Date: March 18th, 2021

DOI: https://doi.org/10.21203/rs.3.rs-298067/v1

Version of Record: A version of this preprint was published at Journal of Molecular Medicine on September 8th, 2021. See the published version at https://doi.org/10.1007/s00109-021-02119-6.

Abstract

Background: Dilated cardiomyopathy (DCM) is the third most common cause of heart failure. The multidisciplinary nature of testing, -involving genetics, imaging, or cardiovascular techniques-, makes its diagnosis challenging. Novel and reliable biomarkers are needed for early identification and tailored personalized management. Peripheral circular RNAs (circRNAs), a leading research topic, remain mostly unexplored in DCM. We aimed to assess whether peripheral circRNAs are expressed differentially among etiology-based DCM. The study was based on a case-control multicentric study.

Methods: We enrolled 130 subjects: healthy controls (n=20), idiopathic DCM (n=30), ischemic DCM (n=20) and familial DCM patients which included pathogen variants of i) *LMNA* gene (n=30) and ii) BCL2-associated athanogene 3 (*BAG3*) gene (n=30). Differentially expressed circRNAs were analyzed in plasma samples by quantitative RT-PCR and correlated to relevant systolic and diastolic parameters. The pathophysiological implications were explored through bioinformatics tools.

Results: Four circRNAs were overexpressed compared to controls: hsa_circ_0003258, hsa_circ_0051238, and hsa_circ_0051239 in *LMNA*-related DCM; and hsa_circ_0089762 in the ischemic DCM cohort. The obtained areas under the curve confirm the discriminative capacity of circRNAs.

Conclusions: The circRNAs correlated with some diastolic and systolic echocardiographic parameters with notable diagnostic potential in DCM. Circulating circRNAs may be helpful for the etiology-based diagnosis of DCM as a non-invasive biomarker.

Introduction

Heart failure is a global pandemic affecting more than 25 million people worldwide, with a continuously increasing prevalence [1]. One of the major causes of heart failure is dilated cardiomyopathy (DCM), characterized by chamber enlargement and contractile dysfunction of the left ventricle (LV) [2]. Several etiologies are included in the DCM common pathway. Ischemic cardiomyopathy is more common than non-ischemic (59% compared with 41%) [2]. Among non-ischemic cardiomyopathy, up to 35% of idiopathic DCM may have a family history [2, 3]. Pathogenic alterations in the gene encoding nuclear lamin A and C proteins-Lamin A/C (*LMNA*) explain 5–10% of familial DCM cases.

DCM is a heterogeneous entity that has different outcomes and may require diverse therapies [4]. Notably, ischemic and familial DCM are major groups with life-threatening arrhythmias [3]. *LMNA*-related DCM presents highly aggressive outcomes and lethal ventricular arrhythmias [5]. Male sex, LV ejection fraction (LVEF) lower than 50%, and non-missense mutations are independent predictors of adverse outcome [6]. Thus, the identification of DCM etiology may help clinicians to stratify patients at risk of fatal events. However, the diagnosis process to reach DCM etiology involves several clinical steps. Multidisciplinary teams, imaging tests, the high cost of genetic testing and its low efficiency makes DCM etiologic diagnosis challenging. A precise, accessible biomarker that supports this process is required to improve diagnosis and early identification of asymptomatic cases. This would facilitate the adoption of tailored management.

Non-coding RNAs have pivotal roles in regulating the network that governs the physiology and pathology of cardiovascular diseases [7]. To date, microRNAs (miRNAs) have been considered a more relevant biomarker candidate due to the complexity of circular RNA (circRNA) assessment in human screening [8]. However, circRNAs also have thought-provoking features. The advantages of circRNAs are their cell type, tissue, and developmental stage specificity. Furthermore, they are independently regulated and more stable than lineal RNA, and they are gathered in cells and human body fluids [8]. CircRNAs modulate gene expression by sponging miRNAs, interacting with RNA-binding proteins (RBPs), and competing with canonical splicing of their pre-mRNA precursor [9]. Research reporting circRNAs as an effective diagnostic and therapeutic biomarker in many diseases has grown exponentially in the last decade. Nevertheless, the potential of using this easy-to-monitor and highly stable marker for stratifying DCM etiologies remains unexplored. Additionally, the experimental and computational analysis of these molecular cross-regulations will propel new insights on DCM [8].

The present study aimed to identify differentially expressed circRNAs in the plasma of patients with DCM of various etiologies such as familial, idiopathic or ischemic.

Material And Methods

Study design

The study was based on a case-control multicentric study. Patient samples and the dataset were collected from several centers (Puerta del Mar University Hospital, Cádiz; Cruz Roja Hospital, Madrid; and Virgen de la Victoria University Hospital, Málaga, Spain). We enrolled 130 subjects distributed in five study groups: healthy controls (n = 20), idiopathic DCM (n = 30), ischemic DCM (n = 20) and familial DCM

patients. The carriers of rare pathogenic variants included were: i) *LMNA* gene (n = 30) and ii) *BCL2-associated athanogene 3* (*BAG*3) gene (n = 30) (Fig. 1).

DCM etiology was determined by three independent clinical cardiologists, who are experts in cardiomyopathies. DCM was defined as either LVEF levels below 50% and/or LV end-diastolic diameter larger than 56 mm [10]. *BAG3* and *LMNA* participants were confirmed genetically and fulfilled the diagnostic clinical criteria for familial DCM [11]. The *LMNA* cohort was subclassified as a carrier of the pathogenic variant, phenotypically negative ($LMNA^{Ph-}$) and genetically and phenotypically positive ($LMNA^{Ph+}$) as previously described [11]. Genetic etiology was ruled out in all idiopathic DCM patients. Ischemic DCM was diagnosed if a precedent of acute myocardial infarction or coronary artery disease was shown, which developed LV remodeling and dysfunction [10]. A transthoracic echocardiography protocol was performed as described previously [11, 12]. The information included anthropometric, clinical, therapeutic, electrocardiographic and echocardiographic data from electronic medical records (Table 1).

Table 1
Study population: anthropometric, clinical and echocardiographic variables

Variable	Healthy Control (N = 20)	Idiopathic (N = 30)	*LMNA*$^{Ph-}$ (N = 12)	*LMNA*$^{Ph+}$ (N = 18)	*BAG3* (N = 30)	Ischemic (N = 20)
Age (years)	42.0 ± 11.0	63.7 ± 8.2	40.6 ± 6.9	38.7 ± 15.0	42.2 ± 14.8	71.1 ± 8.5
Sex (male)	55%	70%	23.1%	42.9%	68.4%	72.2%
BMI (kg/m$^{2)}$	25.1 ± 3.3	26.7 ± 2.6	25.4 ± 2.1	23.6 ± 3.9	27.9 ± 4.9	28.8 ± 4.9
Heart rate (bpm)	65.7 ± 11.9	71 ± 13.9	65.7 ± 5.9	64.3 ± 9.9	73 ± 10	64.6 ± 16.8
Smoker	0%	60%	57.1%	30.8%	26.3%	22.2%
SBP (mm Hg)	114.5 ± 8.7	113.1 ± 11.9	128.4 ± 15.9	123.2 ± 20.9	128.1 ± 13.3	124.3 ± 12.7
DBP (mm Hg)	73.5 ± 8.5	73.1 ± 7.1	81.8 ± 6.1	76.7 ± 17.9	81.1 ± 7.8	72.2 ± 8.6
LVEF (%)	68.8 ± 6.0	30.5 ± 10.2	44.5 ± 5.0	61.0 ± 5.9	49.5 ± 11.9	34.7 ± 7.5
LVEDD (mm)	47.7 ± 4.8	63.0 ± 3.8	58.0 ± 3.4	49.2 ± 12.6	55.6 ± 7.5	58.6 ± 4.8
LVESD (mm)	30.0 ± 6.9	48.1 ± 16.8	43.8 ± 3.1	30.7 ± 6.8	40.4 ± 9.3	44.1 ± 13.2
LA volume (mL/m^2)	17.4 ± 4.3	71.1 ± 25.0	49.3 ± 12.4	41.0 ± 15.5	68.2 ± 25.8	62.1 ± 19.6
LAD (mm)	35.1 ± 5.4	45.2 ± 9.1	40.8 ± 4.3	33.8 ± 6.6	37.6 ± 6.5	40.8 ± 6.1
RV (mm)	28.6 ± 3.5	39.7 ± 6.5	31.7 ± 1.9	28.8 ± 5.2	32.1 ± 7.6	31.4 ± 6.9
TAPSE	22.2 ± 2.7	18.2 ± 6.4	21.6 ± 3.6	21.3 ± 3.5	21.1 ± 5.4	18.8 ± 3.9
MAPSE	18.1 ± 1.6	9.6 ± 2.7	12.1 ± 3.1	16.0 ± 2.6	12.3 ± 3.2	10.6 ± 2.1
E (cm/s)	0.7 ± 0.2	0.7 ± 0.2	0.8 ± 0.1	0.8 ± 0.2	0.8 ± 0.3	0.8 ± 0.2
A (cm/s)	0.6 ± 0.1	0.8 ± 0.3	0.7 ± 0.3	0.5 ± 0.2	0.6 ± 0.2	0.8 ± 0.3
S'sTDI (cm/s)	0.08 ± 0.01	0.06 ± 0.06	0.06 ± 0.01	0.08 ± 0.02	0.08 ± 0.01	0.05 ± 0.01
E´s TDI (cm/s)	0.09 ± 0.03	0.05 ± 0.05	0.07 ± 0.02	0.10 ± 0.04	0.09 ± 0.04	0.05 ± 0.01
A´s TDI (cm/s)	0.10 ± 0.03	0.06 ± 0.02	0.11 ± 0.02	0.09 ± 0.04	0.11 ± 0.03	0.07 ± 0.03
E/E' ratio	7.7 ± 2.1	16.3 ± 8.5	10.2 ± 3.0	7.9 ± 2.2	6.3 ± 1.5	15.0 ± 6.4
NYHA functional class (II-III)	0%	10%	14.3%	15.4%	10.5%	11.1%

All values are expressed as mean ± SEM. Abbreviations: A, atrial systolic transmitral flow wave; A´s TDI, atrial septal mitral annular velocity; *BAG3*, BCL2-associated athanogene 3; BMI, body mass index; DBP, diastolic blood pressure; DCM, dilated cardiomyopathy; E, early diastolic transmitral flow wave; E', early diastolic mitral annular velocity; LA, left atrial; LAD, left atrial dimension; *LMNA, lamin* A/C; *LMNA*$^{Ph-}$, *LMNA* carrier of the pathogenic variant; *LMNA*$^{Ph+}$, *LMNA* carrier phenotypically positive; LVEDD, left ventricular end-diastolic dimension; LVEF, left ventricle ejection fraction; LVESD, left ventricle end-systolic dimension; MAPSE, mitral annular plane systolic excursion; NYHA, New York Heart Association classification; RV, right ventricle; S, positive systolic wave; SBP, systolic blood pressure; TAPSE, tricuspid annular plane systolic excursion; TDI, tissue Doppler imaging

Ethics

The study protocol was approved by the Andalusian Biomedical Research Ethics committee.
The study was performed in full compliance with the Declaration of Helsinki.
All participants provided written informed consent.

Genetic analysis

Genetic analysis was performed as previously described [11]. DNA isolation was undertaken using Chemagic MSM I from whole blood (Chemagic Human Blood). DNA integrity was assessed on 0.8% agarose gel and the quality ratios of absorbance were accomplished using spectrophotometric measurements. dsDNA concentration was determined using fluorometry integrity (Qubit, Life Technologies), and corroborated on 0.8% agarose gel.

Blood collection

Ten milliliters of peripheral blood were collected in K2-ethylenediaminetetraacetic acid tubes (BD) after 10 h overnight fasting. None of the patients were under heparin therapy. The blood was processed within 4 h after isolation, centrifuged (1500 g, 15 min, 4°C), and the plasma layer was aliquoted and stored at -80ºC until further analysis.

Microarray analysis

A screening study was carried out using the Arraystar Human Circular RNA Microarray V2.0 (Arraystar, Inc.). This platform analyzed 36 samples of idiopathic and non-idiopathic DCM subjects. Total RNAs from each sample were obtained using the Arraystar's standard protocols (Arraystar, Inc.). The enriched circRNAs were amplified and transcribed into fluorescent cDNA using a random priming method (Arraystar Super RNA Labeling Kit; Arraystar). The labelled cDNAs were hybridized onto the Arraystar Human circRNA Array V2.0 (Arraystar, Inc.). Once the slides had been washed, they were scanned by the Agilent Scanner G2505C.

RNA isolation and quantitative reverse transcriptase-polymerase chain reaction

Total RNA was isolated from 200 µL of plasma using a miRNeasy Serum/Plasma Kit (Qiagen). RNA was eluted with 20 µL of RNase-free H_2O and stored at -80°C. For the circRNA quantification, circulating RNA preparations were reverse transcribed with a first-strand cDNA synthesis kit (Nzytech, Portugal) using a random primer approach and following the manufacturer's instructions. Previous to reverse transcription, samples were spiked with MS2 RNA (Sigma-Aldrich, Germany), which was used as an internal normalizer. Quantification of selected circRNAs was performed by qRT-PCR using divergent DNA primers designed with the circInteractome algorithm [13] (see **Supplemental Table 1** for primer sequences) in an Applied Biosystems by the qRT-PCR system. Fold-change analysis between sample groups was calculated by the Delta-Ct method.

Functional enrichment

Information about circRNAs is available on the circBase website (http://www.circbase.org/). The Circular RNA Interactome (https://circinteractome.nia.nih.gov/) was used to predict miRNAs and RBPs binding sites. The regulatory network was performed with Navigator software [14]. The set of RBPs common to all the differentially expressed circRNAs was analyzed with STRING: functional protein association networks (https://string-db.org) [15]. The set of miRNAs common to all the differentially expressed circRNAs was analyzed with miRNet 2.0 (https://www.mirnet.ca/miRNet/home.xhtml).

Statistical analysis

Continuous variables are expressed as the mean ± standard deviation. Categorical variables are expressed in frequency and percentage (%). Analysis of variance was applied to compare intergroup circRNAs levels. The Pearson correlation was used to test the link between echocardiographic and clinical variables vs. $\log_2$ circRNAs. In addition, the association between circRNAs and echocardiography parameters was assessed using logistic bivariate regression. Several models were constructed using the Wilcoxon test and iterating combinations between our circRNA candidates, as well as echocardiographic and clinical covariates. The changes in *p*-values of their variables were evaluated by the Wald test and a likelihood ratio. To characterize the diagnostic performance of the circRNAs candidate, ROC curves were applied together with a logistic regression model to determine the AUC, the specificity and sensitivity of the optimal cut-offs. ROC curves were generated by plotting sensitivity against 100-specificity. Data were presented as the AUC and 95% CI. The statistical software package R (www.r-project.org) was used for all analyses.

Results

Analysis of circRNA expression profiles in plasma of DCM patients

A total of 36 idiopathic and non-idiopathic DCM patients were assessed to test the differences in circRNA expression profiles. A total of ten candidate circRNAs (see **Supplementary Table 1**) were obtained from circRNA microarray screening of plasmatic samples (fold change > 2, $p < 0.05$).

Validating the expression of the candidate circRNAs

The expression of the ten circRNA candidates was carried out in plasma samples of each study group, using qRT-PCR. Only *LMNA* and ischemic DCM populations showed differential circRNA expression. Circulating levels of hsa_circ_0051238, hsa_circ_0051239 and hsa_circ_0003258 were highly upregulated in the *LMNA* population compared to healthy controls (Fig. 2). To assess the strength of circRNAs as an early biomarker before the clinical manifestation of malignant ventricular arrhythmias and LV dilation, the *LMNA*-related DCM group was subdivided into *LMNA* pathogenic variant carrier, phenotypically negative ($LMNA^{Ph-}$) and phenotypically positive ($LMNA^{Ph+}$). Circulating hsa_circ_0051238 levels were differentially expressed in the $LMNA^{Ph-}$ population ($p = 0.03$) (Fig. 2A). The hsa_circ_0051239 ($LMNA^{Ph-}$ $p = 0.03$, $LMNA^{Ph+}$ $p = 0.04$) and hsa_circ_0003258 ($LMNA^{Ph-}$ $p = 0.03$, $LMNA^{Ph+}$ $p = 0.03$) plasmatic levels were significantly higher in both *LMNA* groups than in healthy subjects (Fig. 2B-C). Regarding the ischemic DCM cohort, the plasma hsa_circ_0089762 levels were significantly higher ($p = 0.04$) than in healthy subjects (Fig. 2D).

Diagnostic value of the validated circRNAs in a DCM population

The receiver operating characteristic (ROC) area under the curve (AUC) analysis was assessed to investigate the circulating circRNAs diagnostic value in discriminating *LMNA* and ischemic DCM etiology from healthy controls. All individual circRNAs show an AUC ≥ 0.7. The highest AUC values reached by hsa_circ_0089762 that demonstrated an AUC value of 0.92 (95% of confidence intervals [CI] range of specificities are shown in Table 2).

Table 2
Comparisons of single circRNA as predictors of DCM

DCM etiology	circRNA	AUC (95% CI)	Sensitivity (%)	Specificity (%)	*p*
LMNA	hsa_circ_0003258	0.75 (0.56–0.94)	61.53	78.57	0.043
	hsa_circ_0051238	0.71 (0.53–0.88)	70	72.73	0.02
	hsa_circ_0051239	0.73 (0.61–0.93)	83.33	72.23	0.007
Ischemic	hsa_circ_0089762	0.92 (0.77-1)	83.33	72.73	0.006

Abbreviations: AUC, area under the curve; CI, confidence interval; DCM, dilated cardiomyopathy; *LMNA, Lamin* A/C

Association between the expression of circRNAs and the clinical characteristics of the DCM population

The association between circulating circRNAs and echocardiographic and clinical features of DCM patients was also analyzed. As indicated in Table 3, the $LMNA^{Ph-}$ group showed a negative correlation between hsa_circ_0003258 and hsa_circ_0051239 with early diastolic mitral annular velocity (E´s TDI). The $LMNA^{Ph+}$ cohort showed a positive correlation of hsa_circ_0051238 with tissue Doppler imaging (TDI) septal atrial systolic mitral annular velocity (A´s TDI) and a negative correlation of hsa_circ_0051238 and hsa_circ_0051239 with LV outflow tract (LVOT) velocity.

Table 3
Correlation between the echocardiographic variables and individual circRNA for the LMNA cohort

	hsa_circ_0003258				hsa_circ_0051238				hsa_circ_0051239			
	$LMNA^{Ph-}$		$LMNA^{Ph+}$		$LMNA^{Ph-}$		$LMNA^{Ph+}$		$LMNA^{Ph-}$		$LMNA^{Ph+}$	
	Pearson *r*	*p*	Pearson *r*	*p*	Pearson *r*	*p*	Pearson *r*	*p*	Pearson *r*	*p*	Pearson *r*	*p*
A´s TDI (cm/s)	0.191	0.623	0.676	0.324	-0.013	0.965	0.859	0.028	0.051	0.875	0.698	0.190
E´s TDI (cm/s)	-0.685	0.042	-0.413	0.587	-0.523	0.067	-0.157	0.766	-0.722	0.008	-0.253	0.681
LVOT (cm/s)	-0.085	0.856	-0.995	0.064	-0.020	0.963	-0.977	0.004	0.043	0.919	-0.97	0.030

Abbreviations: A´s TDI, atrial septal mitral annular velocity; DCM, dilated cardiomyopathy; E´s TDI, early diastolic mitral annular velocity; *LMNA*, *lamin* A/C; $LMNA^{Ph-}$, *LMNA* carrier of the pathogenic variant; $LMNA^{Ph+}$, *LMNA* carrier phenotypically positive; LVOT, left ventricular outflow tract velocity; TDI, tissue Doppler imaging

An additional study was performed to assess correlations between the echocardiographic and clinical variables and hsa_circ_0089762 for the ischemic DCM population. Hsa_circ_0089762 expression was negatively associated with diastolic blood pressure and LVEF (See Table 4).

Table 4
Correlation between the clinical parameters and hsa_circ_0089762 for ischemic DCM cohort

	hsa_circ_0089762	
	Pearson *r*	*p*
DBP (mm Hg)	-0.84	0.036
LVEF (%)	-0.842	0.036
Abbreviations: DCM, dilated cardiomyopathy; DBP, diastolic blood pressure; LVEF, left ventricle ejection fraction		

To further explore the expression of circRNA-DCM disease association, a logistic regression analysis was carried out in our DCM population (Fig. 3). All three *LMNA* linked circRNAs were significantly related to male gender hsa_circ_0003258, hsa_circ_0051238 and hsa_circ_0051239. In the *LMNA* cohort, the bivariate logistic regression analyses revealed that all LVEF were independently negatively associated with hsa_circ_0003258, hsa_circ_0051238 and hsa_circ_0051239. LV mitral annular plane systolic excursion was independent negatively associated with hsa_circ_0003258, and hsa_circ_0051238. Right ventricle (RV) tricuspid annular plane systolic excursion was only independently negatively associated with hsa_circ_0003258. Pulmonary hypertension (PHT) was independently positively related to hsa_circ_0003258 and hsa_circ_0051239.

In the case of hsa_circ_0089762, the logistic regression analysis showed that its circulating levels within A´s TDI wave or the RV dimension were independent influencing factors for ischemic DCM.

Annotation for circRNA/RBPs interaction

An examination of biological processes related to RBPs, with binding sites for circRNA candidates, reveals a set of possible pathways in which circRNAs play a regulative role. *LMNA* mutation influences the proper development of megakaryocytes resulting in altered platelet production/function[16]. We recovered this *LMNA* effect in the enrichment (GO:0045652), regulation of megakaryocyte differentiation (FDR = 0.0013), and fibroblast growth (GO:0008543), (FDR = 0.0267).

The analysis of the intersection set of RBPs predicted to interact with the selected circRNAs (Fig. 4) shows clear enrichment in proteins involved in the control of transcriptional and translational processes (Table 5). Note the association with the regulation of membrane potential, in which IEF4A3 and FMRP are involved (FDR = 0.045).

Table 5
Pathway analysis main findings: PPI enrichment analysis

Pathway	Overlap	FDR	Genes	Database
Regulation of translation	7/327	2.09e-10	*AGO2,EIF4A3,ELAVL1,FMRP,IGF2BP1,IGF2BP2,IGF2BP3*	*GO*
mRNA binding	7/198	1.31e-12	*AGO2,EIF4A3,ELAVL1,FMRP,IGF2BP1,IGF2BP2,IGF2BP3*	*GO*
Negative regulation of nitrogen compound metabolic process	7/2307	8.81e-06	*AGO2,EIF4A3,ELAVL1,FMRP,IGF2BP1,IGF2BP2,IGF2BP3*	*GO*
Regulation of mRNA stability	5/113	1.05e-08	*ELAVL1,FMRP,IGF2BP1,IGF2BP2,IGF2BP3*	*GO*
mRNA transport	5/148	3.12e-08	*EIF4A3,FMRP,IGF2BP1,IGF2BP2,IGF2BP3*	*GO*
Regulation of gene silencing by miRNA	3/78	3.82e-05	*AGO2,ELAVL1,FMRP*	*GO*
Regulation of membrane potential	2/408	0.0445	*EIF4A3,FMRP*	*GO*
MAPK6/MAPK4 signaling	2/86	0.0077	*AGO2,IGF2BP1*	*GO*
ncRNA processing	2/340	0.0344	*AGO2,EIF4A3*	*GO*

Abbreviations: FDR, false discovery rate; GO, gene ontology: KW, keyword

PPI enrichment p-value:1.67e-10

Supplementary Table 1: primer sequences for circRNA quantification by qRT-PCR

circRNA		Forward primer	Reverse primer	Amplicon
(circBase)	Host gene			size
hsa_circ_0089762	JA760602	GGCGTGATCATGAAAGGTG	GGCCACCAATGGTACTGAAC	177
hsa_circ_0051239	ATP5SL	ACACACACACACACGCACAC	AAGACCAAATCCCACATCCTC	120
hsa_circ_0051238	ATP5SL	ACACACACACACACGCACAC	TTCTTCTGATTGCCCTCTGG	128
hsa_circ_0060144	PHF20	GAACCGACTTCTCCCCTTGT	CCCACTTCAAAGCTGATTCC	128
hsa_circ_0059760	TM9SF4	GCCATGTTCATCGAGCTCTT	CCTCCATGGTGTCTTCAATG	120
hsa_circ_0035957	DENND4A	ACCACACACGTTCTGCAAAG	ACCGAAAGTTTCTCTCTGAAAAAG	120
hsa_circ_0003258	ZNF652	TGGGCACAAACAGTTCATGT	TGCGTTTGAATGATTTTCCA	143
hsa_circ_0089761	JA760602	GGCGTGATCATGAAAGGTG	CCCTAGCCAACCCCTTAAAC	136
hsa_circ_0023988	NOX4	CTGCTGACGTTGCATGTTTC	TCGGAGGTAAGCCAAGAGTG	122
hsa_circ_0089763	JA760600	TATGGTGGGCCATACGGTAG	CTCCACCTCCATCATCACCT	136

The analysis of miRNAs sponged by validated circRNAs offers various candidates for further research. Hsa_circ_0003258 has only one functional binding site to hsa-miR-653. As a counterpart, hsa_circ_0051238 and hsa_circ_0051239 present a clear sponge effect over hsa-miR-210, with five binding sites that have ΔU below zero. Thereby, overexpression of hsa_circ_0051238 and hsa_circ_0051239 will actively reduce the availability of hsa-miR-210. Hsa-miR-210 regulates expression of hepatocyte growth factor gene, whose overexpression is considered a treatment for DCM [17]. Additionally, they also present a functional binding site for hsa-miR-330-5p that is involved in cardiomyocyte survival and function recovery [18]. Regarding miRNA-related diseases, hsa_circ_0051238 sponges hsa-miR-873 and hsa-miR-513a-5p are both related with heart disease ($p = 0.075$), and hsa-miR-377 is related with ischemic cardiomyopathy ($p = 0.221$). Hsa_circ_0089762 has sponge activity with multiple, energetically favorable binding sites. Of note is hsa-miR-21, as well as hsa-miR-183,

hsa-miR-361-3p, hsa-miR-384, hsa-miR-873, hsa-miR-938, hsa-miR-1249 and hsa-miR-1283. The miRNAs sponged by the circRNAs with a context score over 90% was used to capture the set of mRNAs regulated by these miRNAs. Functional enrichment, using a hypergeometric association algorithm, shows that 148 proteins of the network were related with focal adhesion ($p = 2.68e^{-8}$) and 128 proteins were linked with regulation of the actin cytoskeleton (p = 0.00002). Gene ontology biological processes, using the same hypergeometric algorithm, show a significant correlation with endoplasmic reticulum-nuclei signaling pathways ($p = 0.1e^{-6}$) and pre- and post-Golgi vesicle transportation ($p = 8.6e^{-7}$ and $4.47e^{-7}$ respectively).

Discussion

Over the last decade, the diagnostic process of DCM etiologies has focused on searching for new biomarkers. An efficient biomarker for DCM should be robust, stable, non-invasive, sensitive, specific to this entity, predictive of a particular DCM etiology, and show a preclinical and clinical relevance to be validated in animal and/or human cell models [19]. We propose the use of peripheral circRNAs as a novel discriminant biomarker of DCM etiologies.

Unlike linear RNA, single circulating circRNAs or circRNAs combined with various other biomarkers are a promising tool for clinical diagnosis of heart diseases, which would improve outcome [20]. Thus, circRNA MICRA was reported to risk-stratify patients after acute myocardial infarction [21]. Peripheral circ_0124644 and circ_0098964 levels have been described as a diagnostic biomarker of coronary artery disease [22]. Related to cardiomyopathies, a set of circulating circRNAs DNAJC6, TMEM56 and MBOAT2 has been proposed to discriminate between healthy and hypertrophic cardiomyopathy [23]. In this sense, hsa_circ_0071542 was upregulated in children with fulminant myocarditis in leukocytes isolated from peripheral blood [24]. Nevertheless, this area remains mostly unexplored in DCM [22, 25]. Hence, further analysis of circRNAs among DCM etiologies might provide early, precise characterization of the disease and lead to novel pathological information, beyond the traditional biomarkers. To the best of our knowledge, the present study is the first to describe a subset of circulating circRNA for a discriminative etiology-based diagnostic in DCM. Circulating hsa_circ_0003258, hsa_circ_0051238 and hsa_circ_0051239 expression levels were upregulated in *LMNA*-related DCM patients. Notably, hsa_circ_0051238 plasmatic levels were significantly present in the $LMNA^{Ph-}$ cohort. Hence, it may be a promising diagnostic biomarker for the early identification of patients in an initial stage of *LMNA*-related DCM. This will allow personalized therapeutic measures to be applied that help to improve the progression and outcome of *LMNA*-related DCM. Furthermore, plasmatic hsa_circ_0089762 may provide discriminative power for the ischemic DCM cohort with high-yield diagnostic accuracy and an AUC of 0.92. These circRNAs have been identified mostly in various types of oncologic processes [26–31]. Thus, only hsa_circ_0051239 levels have been upregulated in the myocardium of congenital ventricular septal defect [31]. However, they have not been previously described in DCM cases.

In the current study, circRNA were related to clinical and echocardiographic variables. Male gender, rare non-missense variants in *LMNA*, and LVEF < 50% have been established as independent factors associated with a more aggressive outcome and even death during follow-up [32]. Herein, all three circRNAs associated with *LMNA*-DCM etiology were related to male gender [33]. On the other side, echocardiography variables and related circRNAs might suggest a time-evolving sequence. TDI echocardiography is a non-invasive, very sensitive method to assess the cardiac hemodynamic in DCM [34]. TDI reveals that subtle impairment in diastolic myocardial tissue velocities are markers of early cardiac disease and have been associated with outcome in various cardiopathies [16, 17]. In the $LMNA^{Ph-}$ group, the E´s TDI is negatively related to hsa_circ_0003258 and hsa_circ_0051239. This E´s TDI impairment suggests an underlying early diastolic dysfunction [35]. A´s TDI in the $LMNA^{Ph+}$ group showed a positive correlation, which indicates that the left atrium is a prominent factor to maintain the LV filling pressure when diastolic dysfunction advances. This sequential TDI septal impairment mirrors the transition from $LMNA^{Ph-}$ to $LMNA^{Ph+}$ and may be related to the progressive fibrosis of the interventricular septum located in the basal portion, which is characteristic of the *LMNA* related-DCM that has been associated with ventricular arrhythmias and worse prognosis [36]. LVEF was independently negatively associated with hsa_circ_0003258, hsa_circ_0051238 and hsa_circ_0051239. According to the LV systolic impairment, hsa_circ_0003258 and hsa_circ_0051238 were related to LV mitral annular plane systolic excursion. Thus, changes in contractility quantified by LV mitral annular plane systolic excursion occur as compensatory mechanisms before impairment of ventricular function [37]. Hsa_circ_0051238 and hsa_circ_0051239 were also negatively related to LVOT velocity, which suggests progressive impairment of the cardiac pump in the $LMNA^{Ph+}$ cohort. Dysfunction of RV is a final common step in DCM and heart failure [38]. RV pressure overload due to PHT, the interventricular interdependence affected by septal fibrosis and underlying ischemia may influence this situation. In support of our results, circRNA, hsa_circ_0003258 was positively increased with the RV lower tricuspid annular plane systolic excursion and PHT [39].

Otherwise, hsa_circ_0089762 correlated to diastolic blood pressure and LVEF in the ischemic group, which supports our results as a specific, highly sensitive biomarker with high-yield diagnostic accuracy. Moreover, hsa_circ_0089762 was related to A´s TDI, which suggests more advanced progression of this entity. Its association with an increase in RV dimension could add information for tailored management in this

group, since RV impairment is a worse outcome marker in the ischemic population [40]. In addition, RV involvement has a multifactorial origin that may be influenced by LV remodelling, increased LV filling pressures, the appearance of PHT or RV ischemia [41].

Regarding biological implications, circRNAs spring from introns or exons of their parental genes by back-spliced circularization [25]. Hence, the ratio between linear and circular fractions affects gene expression. According to the protein atlas (proteinatlas.org), parental genes are expressed in cardiac tissue, which supports correlations between etiologies and circRNAs. Hsa_circ_0003258 is synthesized from *ZNF652* gene. ZNF652 interacts with CBFA2T3, which acts as a transcriptional repressor [42]. *ZNF652* is associated with systolic or diastolic blood pressure and hypertension. However, its role remains unclear [43]. Hsa_circ_0051238 and hsa_circ_0051239 come from the *ATP5SL* gene. *ATP5SL* is required for the assembly of mitochondrial NADH: ubiquinone oxidoreductase complex (complex I). Complex I is essential to provide the energy for cardiac function and is related to DCM progression [44]. *ATP5SL* has been associated with a congenital ventricular septal defect by the overexpression of hsa_circ_0051239 [45]. Finally, hsa_circ_0089762 is generated from the *MT-CO2* gene. MT-CO2 is part of the electron transport chain of the mitochondria. Reduced activity of the electron transport chain subunits has been described independently of etiology in ischemic or idiopathic DCM patients [46].

The functional enrichment of the intersecting set of RBSs reveals the role of FMRP in regulation of the membrane potential. Bao *et al.* described FMRP isoform 1, in rats, as an essential protection factor and a novel potential biomarker in the cardiovascular system[47]. The participation of circRNAs in regulatory networks involving competing-endogenous RNA interactions by sequestering miRNAs has been characterized recently in cardiovascular pathologies [48, 49]. From the set of miRNAs that could be sponged by the circRNAs that we considered, we found significant enrichment in the regulation of focal adhesion and actin cytoskeleton. Both have an important role in human DCM [50], which suggests new pathways of study.

Our current study has several limitations. Firstly, our sample was prospectively recruited from the outpatient clinic. The size of the study sample, comprised of strictly DCM patients, did not allow us to obtain a robust multivariate logistic regression model. In consequence, these results should be extended and replicated to a larger population before the novel biomarkers can be routinely applied in clinical practice. Furthermore, data on natriuretic peptides or troponin were not accessible for all patients. Finally, even though databases registered the expression of the parental genes in cardiac tissue, we have no confirmation about the direct secretion from the heart of these circulating circRNAs into the extracellular space. Hence, the association of circRNAs with DCM and all the interactions are putative. Further analysis should be carried out on human heart samples to confirm our results.

Conclusion

Exploring new biomarkers through circular transcriptome expression patterns will identify new targets in DCM pathogenesis. We propose a circulating circRNAs fingerprint to discriminate between various DCM etiologies. Circulating hsa_circ_0003258, hsa_circ_0051238 and hsa_circ_0051239 expression levels are higher in *LMNA*-related DCM, and hsa_circ_0089762 levels are specifically upregulated in the ischemic DCM cohort. These circulating circRNAs and certain echocardiographic variables might improve the etiology-based diagnostic, allow early identification of asymptomatic cases and tailored-treatment of the DCM population.

Abbreviations

A´s TDI Atrial septal mitral annular velocity

AUC Area under the curve

BAG3 BCL2-associated athanogene 3

CI Confidence interval

circRNA Circular RNA

DCM Dilated cardiomyopathy

E´s TDI Early diastolic mitral annular velocity

FDR False discovery rate

LMNA Lamin A/C

LV Left ventricular

LVEF LV ejection fraction

LVOT LV outflow tract

MAPSE Mitral annular plane systolic excursion

mRNA Messenger RNA

miRNA MicroRNA

PHT Pulmonary hypertension

ROC Receiver operating characteristic

RBP RNA binding protein

qRT-PCR Quantitative real-time polymerase chain reaction

TAPSE Tricuspid annular plane systolic excursion

TDI Tissue Doppler imaging

Declarations

DECLARATIONS: We know of no conflicts of interest associated with this publication, and there has been no significant financial support for this work that could have influenced its outcome. The study protocol was approved by the Andalusian Biomedical Research Ethics committee. The study was performed in full compliance with the Declaration of Helsinki. Informed consent was obtained from all subjects involved in the study. Written in-formed consent has been obtained from the patients for paper publication.

CONSENT TO PARTICIPATE/FOR PUBLICATIONS: Informed consent was obtained from all subjects involved in the study. Written in-formed consent has been obtained from the patients for paper publication.

AVAILABILITY OF DATA AND MATERIAL: data transparency is guaranteed. The datasets generated during and/or analysed during the current study are available from the corresponding author on reasonable request.

CODE AVAILABILITY: We used various softwares for functional enrichment and statistical analysis. All of them are cited in our manuscript.

CONFLICTS OF INTEREST/COMPETING INTERESTS: We know of no conflicts of interest associated with this publication, and there has been no significant financial support for this work that could have influenced its outcome.

FUNDING: This work was supported by grants in the framework of the European Regional Development Fund (ERDF) Integrated Territorial Initiative (ITI PI0048-2017 and ITI0033_2019), the Fundación Pública Andaluza Progreso y Salud (FPS00136-2018), a clinical research grant from the Spanish Society of Cardiology for Basic Research in cardiology (PI0012_2019), Plan Propio de INIBICA (PI-INBICA 2019-13), COST (European Cooperation in Science and Technology) Action EUCardioRNA CA17129 and the Portuguese Foundation for Science and Technology (FCT) under the framework of the research grant PTDC-MED-GEN-29389-2017.

AUTHOR CONTRIBUTIONS: All authors have read and approved the submission of the manuscript. Author Con-tributions: Calderon-Dominguez M, Mangas A and Toro R conceived the experiments, Quezada-Feijoo M, Ramos M, Campuzano O, Sarquellas Brugada- G, Pinilla JM, Robles Mezcua A, Mangas A, Toro R recruited the subjects, Thalia extracted RNA from samples,. Costa M, Calderon-Dominguez M, Enguita FJ and Toro R conducted the experiments, and analysed the results. Calderon-Dominguez M, Mangas A and Toro R wrote the manuscript. All au-thors reviewed the manuscript.

ACKNOWLEDGEMENTS

This work is supported by the Fundación Pública Andaluza Progreso y Salud para la Financiación, co-financed by the European Regional Development Fund (ERDF) (PI-0048-2017 and 0017-2019), Plan Propio de INIBICA (PI-INBICA 2019-13), Fundación Pública Andaluza Progreso y Salud (PI 0136-2018), COST (European Cooperation in Science and Technology) Action EUCardioRNA CA17129 and the Portuguese Foundation for Science and Technology (FCT) under the framework of the research grant PTDC-MED-GEN-29389-2017. The

study was also supported by a grant from the Spanish Society of Cardiology for Basic Research (0011-2019). We would like to thank Galan Pacheco for statistical support. We would also like to thank all patients involved in this project.

References

1. Savarese G, Lund LH (2017) Global Public Health Burden of Heart Failure. Card Fail Rev 03:7. https://doi.org/10.15420/cfr.2016:25:2
2. McNally EM, Mestroni L (2017) Dilated cardiomyopathy: Genetic determinants and mechanisms. Circ Res 121:731–748. https://doi.org/10.1161/CIRCRESAHA.116.309396
3. Rosenbaum AN, Agre KE, Pereira NL (2020) Genetics of dilated cardiomyopathy: practical implications for heart failure management. Nat Rev Cardiol 17:286–297
4. Van Der Bijl P, Delgado V, Bootsma M, Bax JJ (2018) Risk stratification of genetic, dilated cardiomyopathies associated with neuromuscular disorders. Circulation 137:2514–2527. https://doi.org/10.1161/CIRCULATIONAHA.117.031110
5. Domínguez F, Cuenca S, Bilińska Z et al (2018) Dilated Cardiomyopathy Due to BLC2-Associated Athanogene 3 (BAG3) Mutations. J Am Coll Cardiol 72:2471–2481. https://doi.org/10.1016/j.jacc.2018.08.2181
6. Kumar S, Baldinger SH, Gandjbakhch E et al (2016) Long-Term Arrhythmic and Nonarrhythmic Outcomes of Lamin A/C Mutation Carriers. J Am Coll Cardiol 68:2299–2307. https://doi.org/10.1016/j.jacc.2016.08.058
7. Lu D, Thum T (2019) RNA-based diagnostic and therapeutic strategies for cardiovascular disease. Nat Rev Cardiol 16:661–674
8. Memczak S, Papavasileiou P, Peters O, Rajewsky N (2015) Identification and Characterization of Circular RNAs As a New Class of Putative Biomarkers in Human Blood. PLoS One 10:e0141214. https://doi.org/10.1371/journal.pone.0141214
9. Stepien E, Costa MC, Kurc S et al (2018) The circulating non-coding RNA landscape for biomarker research: Lessons and prospects from cardiovascular diseases review-article. Acta Pharmacol Sin 39:1085–1099. https://doi.org/10.1038/aps.2018.35
10. Elliott P, Andersson B, Arbustini E et al (2008) Classification of the cardiomyopathies: A position statement from the european society of cardiology working group on myocardial and pericardial diseases. Eur Heart J 29:270–276. https://doi.org/10.1093/eurheartj/ehm342
11. Belmonte T, Mangas A, Calderon-Dominguez M et al (2020) Peripheral microRNA panels to guide the diagnosis of familial cardiomyopathy. Transl Res 218:1–15. https://doi.org/10.1016/j.trsl.2020.01.003
12. Toro R, Blasco-Turrión S, Morales-Ponce FJ et al (2018) Plasma microRNAs as biomarkers for Lamin A/C-related dilated cardiomyopathy. J Mol Med 96:845–856
13. Dudekula DB, Panda AC, Grammatikakis I et al (2016) Circinteractome: A web tool for exploring circular RNAs and their interacting proteins and microRNAs. RNA Biol 13:34–42. https://doi.org/10.1080/15476286.2015.1128065
14. Shirdel EA, Xie W, Mak TW, Jurisica I (2011) NAViGaTing the Micronome – Using Multiple MicroRNA Prediction Databases to Identify Signalling Pathway-Associated MicroRNAs. PLoS One 6:e17429. https://doi.org/10.1371/journal.pone.0017429
15. Szklarczyk D, Gable AL, Lyon D et al (2019) STRING v11: Protein-protein association networks with increased coverage, supporting functional discovery in genome-wide experimental datasets. Nucleic Acids Res 47:D607–D613. https://doi.org/10.1093/nar/gky1131
16. Izquierdo I, Rosa I, Bravo SB et al (2016) Proteomic identification of putative biomarkers for early detection of sudden cardiac death in a family with a LMNA gene mutation causing dilated cardiomyopathy. J Proteomics 148:75–84. https://doi.org/10.1016/j.jprot.2016.07.020
17. Komamura K, Tatsumi R, Miyazaki J et al (2004) Treatment of dilated cardiomyopathy with electroporation of hepatocyte growth factor gene into skeletal muscle. Hypertens (Dallas, Tex 1979) 44:365–71. https://doi.org/10.1161/01.HYP.0000139916.96375.47
18. Van Rooij E, Sutherland LB, Liu N et al (2006) A signature pattern of stress-responsive microRNAs that can evoke cardiac hypertrophy and heart failure. Proc Natl Acad Sci U S A 103:18255–18260. https://doi.org/10.1073/pnas.0608791103
19. Martín-Ventura JL, Blanco-Colio LM, Tuñón J et al (2009) Biomarkers in Cardiovascular Medicine. Rev Española Cardiol (English Ed 62:677–688. https://doi.org/10.1016/s1885-5857(09)72232-7
20. Khan MAF, Reckman YJ, Aufiero S et al (2016) RBM20 Regulates Circular RNA Production from the Titin Gene. Circ Res 119:996–1003. https://doi.org/10.1161/CIRCRESAHA.116.309568
21. Salgado-Somoza A, Zhang L, Vausort M, Devaux Y (2017) The circular RNA MICRA for risk stratification after myocardial infarction. IJC Hear Vasc 17:33–36. https://doi.org/10.1016/j.ijcha.2017.11.001
22. Zhao Z, Li X, Gao C et al (2017) Peripheral blood circular RNA hsa-circ-0124644 can be used as a diagnostic biomarker of coronary artery disease. Sci Rep 7:1–9. https://doi.org/10.1038/srep39918
23. Sonnenschein K, Wilczek AL, de Gonzalo-Calvo D et al (2019) Serum circular RNAs act as blood-based biomarkers for hypertrophic obstructive cardiomyopathy. Sci Rep 9:1–8. https://doi.org/10.1038/s41598-019-56617-2

24. Zhang L, Han B, Wang J et al (2019) Differential expression profiles and functional analysis of circular RNAs in children with fulminant myocarditis. Epigenomics 11:1129–1141. https://doi.org/10.2217/epi-2019-0101
25. Gabriel AF, Costa MC, Enguita FJ (2020) Circular RNA-centered regulatory networks in the physiopathology of cardiovascular diseases. Int. J. Mol. Sci. 21
26. Guo J, Duan H, Li Y et al (2019) A novel circular RNA circ-ZNF652 promotes hepatocellular carcinoma metastasis through inducing snail-mediated epithelial-mesenchymal transition by sponging miR-203/miR-502-5p. Biochem Biophys Res Commun 513:812–819. https://doi.org/10.1016/j.bbrc.2019.03.214
27. Fu C, Lv R, Xu G et al (2017) Circular RNA profile of infantile hemangioma by microarray analysis. PLoS One 12:1–16. https://doi.org/10.1371/journal.pone.0187581
28. Mo WL, Jiang JT, Zhang L et al (2020) Circular RNA hsa_circ_0000467 Promotes the Development of Gastric Cancer by Competitively Binding to MicroRNA miR-326-3p. Biomed Res Int 2020:. https://doi.org/10.1155/2020/4030826
29. Wu Z, Sun H, Wang C et al (2020) Mitochondrial Genome-Derived circRNA mc-COX2 Functions as an Oncogene in Chronic Lymphocytic Leukemia. Mol Ther - Nucleic Acids 20:801–811. https://doi.org/10.1016/j.omtn.2020.04.017
30. Yavropoulou M, Poulios C, Michalopoulos N et al (2018) A Role for Circular Non-Coding RNAs in the Pathogenesis of Sporadic Parathyroid Adenomas and the Impact of Gender-Specific Epigenetic Regulation. Cells 8:15. https://doi.org/10.3390/cells8010015
31. Xu C, Yu Y, Ding F (2018) Microarray analysis of circular RNA expression profiles associated with gemcitabine resistance in pancreatic cancer cells. Oncol Rep 40:395–404. https://doi.org/10.3892/or.2018.6450
32. Van Rijsingen IAW, Arbustini E, Elliott PM et al (2012) Risk factors for malignant ventricular arrhythmias in Lamin A/C mutation carriers: A European cohort study. J Am Coll Cardiol 59:493–500. https://doi.org/10.1016/j.jacc.2011.08.078
33. van Rijsingen IAW, Nannenberg EA, Arbustini E et al (2013) Gender-specific differences in major cardiac events and mortality in lamin A/C mutation carriers. Eur J Heart Fail 15:376–384. https://doi.org/10.1093/eurjhf/hfs191
34. Van Rijsingen IAW, Bakker A, Azim D et al (2013) Lamin A/C mutation is independently associated with an increased risk of arterial and venous thromboembolic complications. Int J Cardiol 168:472–477. https://doi.org/10.1016/j.ijcard.2012.09.118
35. Pérez-Serra A, Toro R, Campuzano O et al (2015) A novel mutation in lamin A/C causing familial dilated cardiomyopathy associated with sudden cardiac death. J Card Fail 21:217–225. https://doi.org/10.1016/j.cardfail.2014.12.003
36. Fontana M, Barison A, Botto N et al (2013) CMR-Verified Interstitial Myocardial Fibrosis as a Marker of Subclinical Cardiac Involvement in LMNA Mutation Carriers. JACC Cardiovasc Imaging 6:124–126. https://doi.org/10.1016/j.jcmg.2012.06.013
37. Hernandez-Suarez DF, Lopez-Menendez F, Roche-Lima A, Lopez-Candales A (2019) Assessment of Mitral Annular Plane Systolic Excursion in Patients With Left Ventricular Diastolic Dysfunction. Cardiol Res 10:83–88. https://doi.org/10.14740/cr837
38. Rudski LG, Lai WW, Afilalo J et al (2010) Guidelines for the Echocardiographic Assessment of the Right Heart in Adults: A Report from the American Society of Echocardiography. Endorsed by the European Association of Echocardiography, a registered branch of the European Society of Cardiology, and. J Am Soc Echocardiogr 23:685–713
39. Merlo M, Gobbo M, Stolfo D et al (2016) The Prognostic Impact of the Evolution of RV Function in Idiopathic DCM. JACC Cardiovasc Imaging 9:1034–1042. https://doi.org/10.1016/j.jcmg.2016.01.027
40. Brieke A, DeNofrio D (2005) Right ventricular dysfunction in chronic dilated cardiomyopathy and heart failure. Coron Artery Dis 16:5–11. https://doi.org/10.1097/00019501-200502000-00002
41. Kukulski T, She L, Racine N et al (2015) Implication of right ventricular dysfunction on long-term outcome in patients with ischemic cardiomyopathy undergoing coronary artery bypass grafting with or without surgical ventricular reconstruction. J Thorac Cardiovasc Surg 149:1312–1321. https://doi.org/10.1016/j.jtcvs.2014.09.117
42. Kumar R, Selth LA, Schulz RB et al (2011) Genome-wide mapping of ZNF652 promoter binding sites in breast cancer cells. J Cell Biochem 112:2742–2747. https://doi.org/10.1002/jcb.23214
43. Korkor MT, Meng FB, Xing SY et al (2011) Microarray analysis of differential gene expression profile in peripheral blood cells of patients with human essential hypertension. Int J Med Sci 8:168–179. https://doi.org/10.7150/ijms.8.168
44. Jarreta D, Orús J, Barrientos A et al (2000) Mitochondrial function in heart muscle from patients with idiopathic dilated cardiomyopathy. Cardiovasc Res 45:860–865. https://doi.org/10.1016/S0008-6363(99)00388-0
45. Liu H, Hu Y, Zhuang B et al (2018) Differential expression of CircRNAs in embryonic heart tissue associated with ventricular septal defect. Int J Med Sci 15:703–712. https://doi.org/10.7150/ijms.21660
46. Govindaraj P, Rani B, Sundaravadivel P et al (2019) Mitochondrial genome variations in idiopathic dilated cardiomyopathy. Mitochondrion 48:51–59. https://doi.org/10.1016/j.mito.2019.03.003

47. Bao J, Ye C, Zheng Z, Zhou Z (2018) Fmr1 protects cardiomyocytes against lipopolysaccharide–induced myocardial injury. Exp Ther Med 16:1825–1833. https://doi.org/10.3892/etm.2018.6386
48. Wang K, Gan TY, Li N et al (2017) Circular RNA mediates cardiomyocyte death via miRNA-dependent upregulation of MTP18 expression. Cell Death Differ 24:1111–1120. https://doi.org/10.1038/cdd.2017.61
49. Costa MC, Cortez-Dias N, Gabriel A et al (2019) circRNA-miRNA cross-talk in the transition from paroxysmal to permanent atrial fibrillation. Int J Cardiol 290:134–137. https://doi.org/10.1016/j.ijcard.2019.04.072
50. Towbin JA (1998) The role of cytoskeletal proteins in cardiomyopathies. Curr Opin Cell Biol 10:131–139. https://doi.org/10.1016/S0955-0674(98)80096-3

Figures

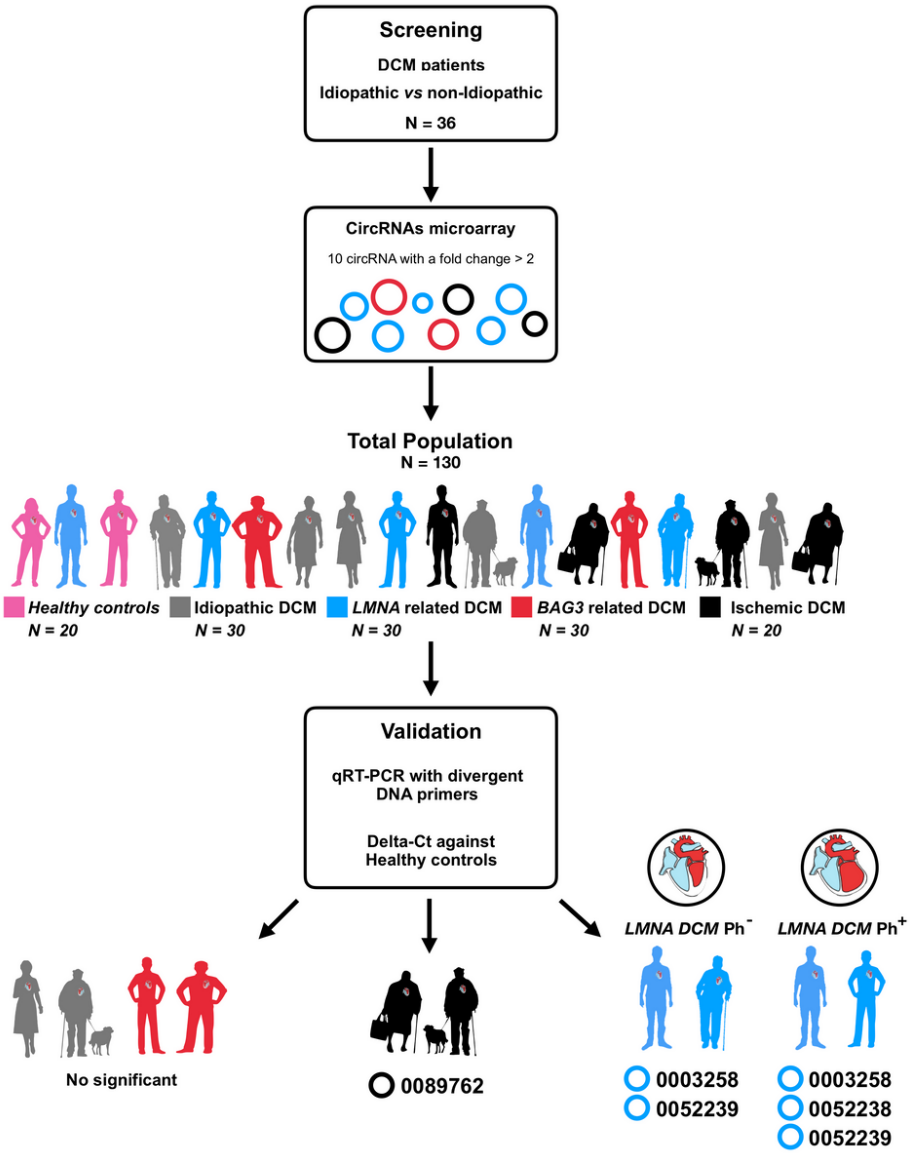

Figure 1

Flowchart of the study design strategy. This figure illustrates the experimental workflow of the study including screening, validation and peripherial circRNAs overexpressed for the LMNAPh-, LMNAPh+ and ischemic DCM cohort. Abbreviations: BAG3, BCL2-associated athanogene 3; DCM, dilated cardiomyopathy; lamin A/C; LMNAPh-, LMNA carrier of the pathogenic variant; LMNAPh+, LMNA carrier phenotype positive; LVEF, left ventricle ejection fraction.

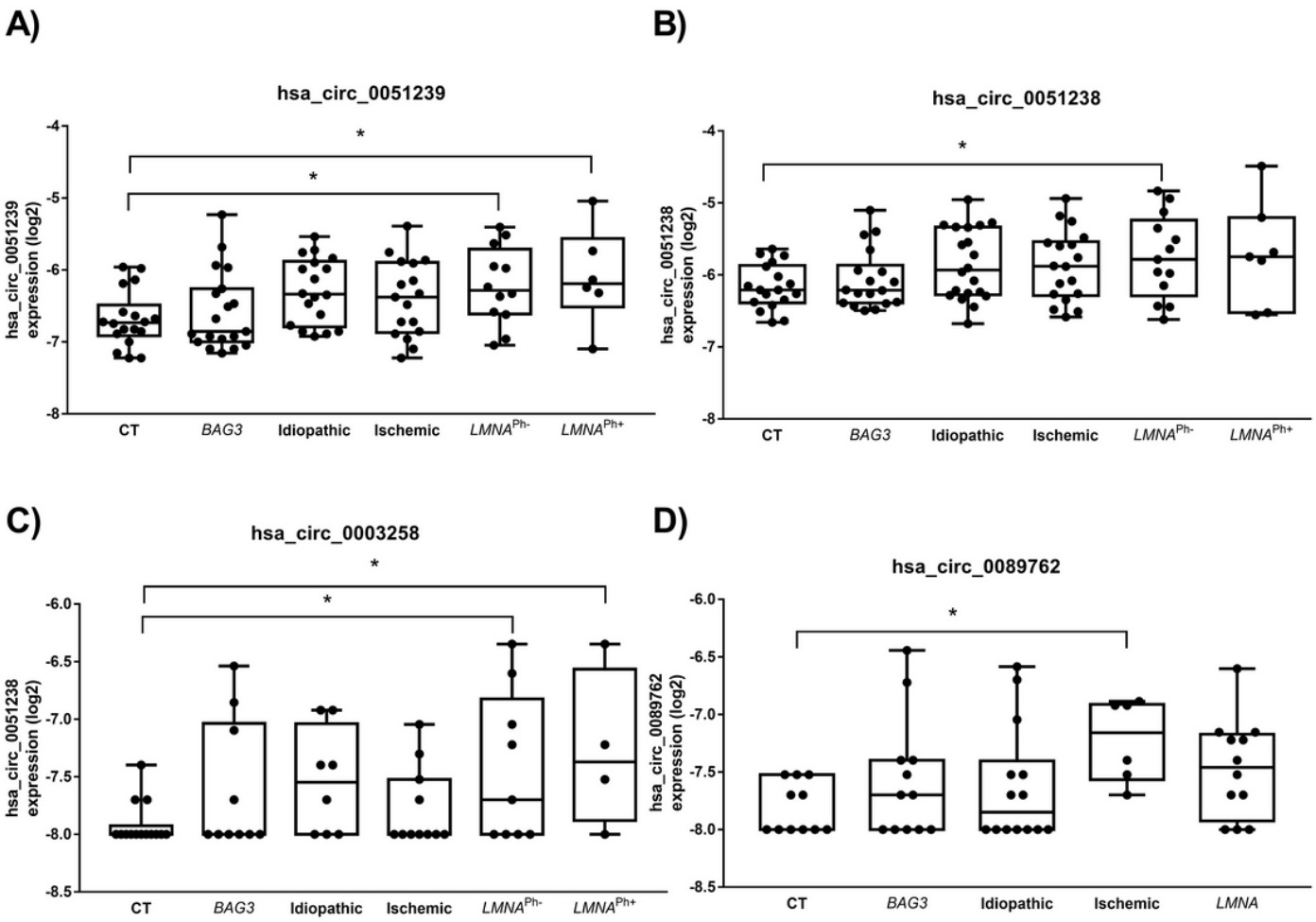

Figure 2

Boxplots of circRNA expression levels, normalized to MS2 RNA, in healthy subjects, BAG3-related DCM, idiopathic DCM, ischemic DCM and LMNA-related DCM. The analysis was carried out using qRT-PCR. Data are present in log2. Data represent the mean ± SEM. *p <0.05. Abbreviations: BAG3, BCL2-associated athanogene 3; CT, healthy cohort; circRNA, circular RNA; DCM, dilated cardiomyopathy; LMNA, lamin A/C; LMNAPh-, LMNA carrier of the pathogenic variant; LMNAPh+, LMNA carrier phenotype positive.

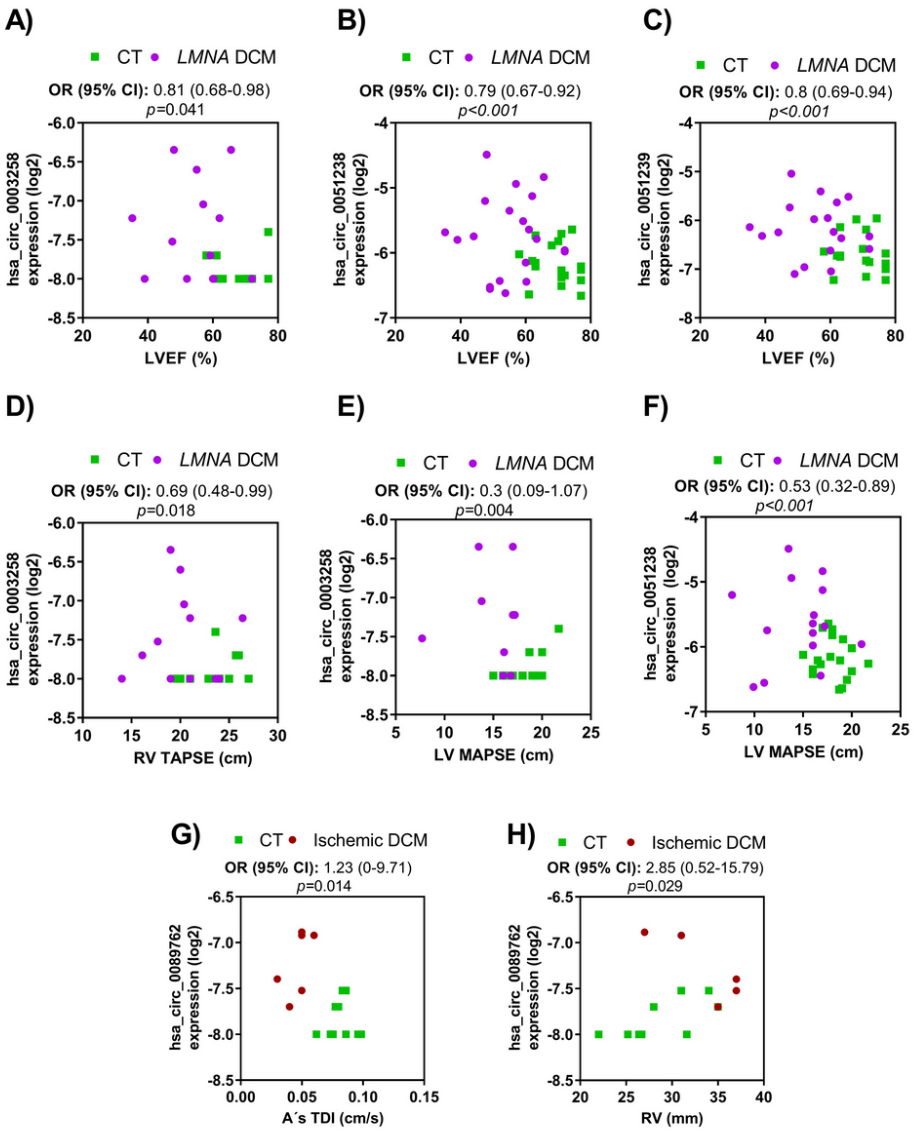

Figure 3

Bivariate logistic regression analysis for LMNA-related DCM and ischemic DCM patients. (A-F) Logistic regression analysis for the LMNA-related DCM cohort. LVEF was independently negatively related with hsa_circ_0003258 (A), hsa_circ_0051238 (B) and hsa_circ_0051239 (C). (D) RV tricuspid annular plane systolic excursion (TAPSE) was negatively related to hsa_circ_0003258. (E-F) LV mitral annular plane systolic excursion (MAPSE) was negatively correlated with hsa_circ_0003258 and hsa_circ_0051238. (G-H) The levels of hsa_circ_0089762 were associated with A´s TDI (G) and RV (H). The odds ratio, 95% of CI and p values are indicated for each logistic regression analysis. Abbreviations: A´s TDI, atrial septal mitral annular velocity; CT, healthy group; CI, confidence intervals; LMNA, lamin A/C gene; LVEF, left ventricle ejection fraction; MAPSE, mitral annular plane systolic excursion; OR, odd ratio; RV; right ventricle; TAPSE, tricuspid annular plane systolic excursion.

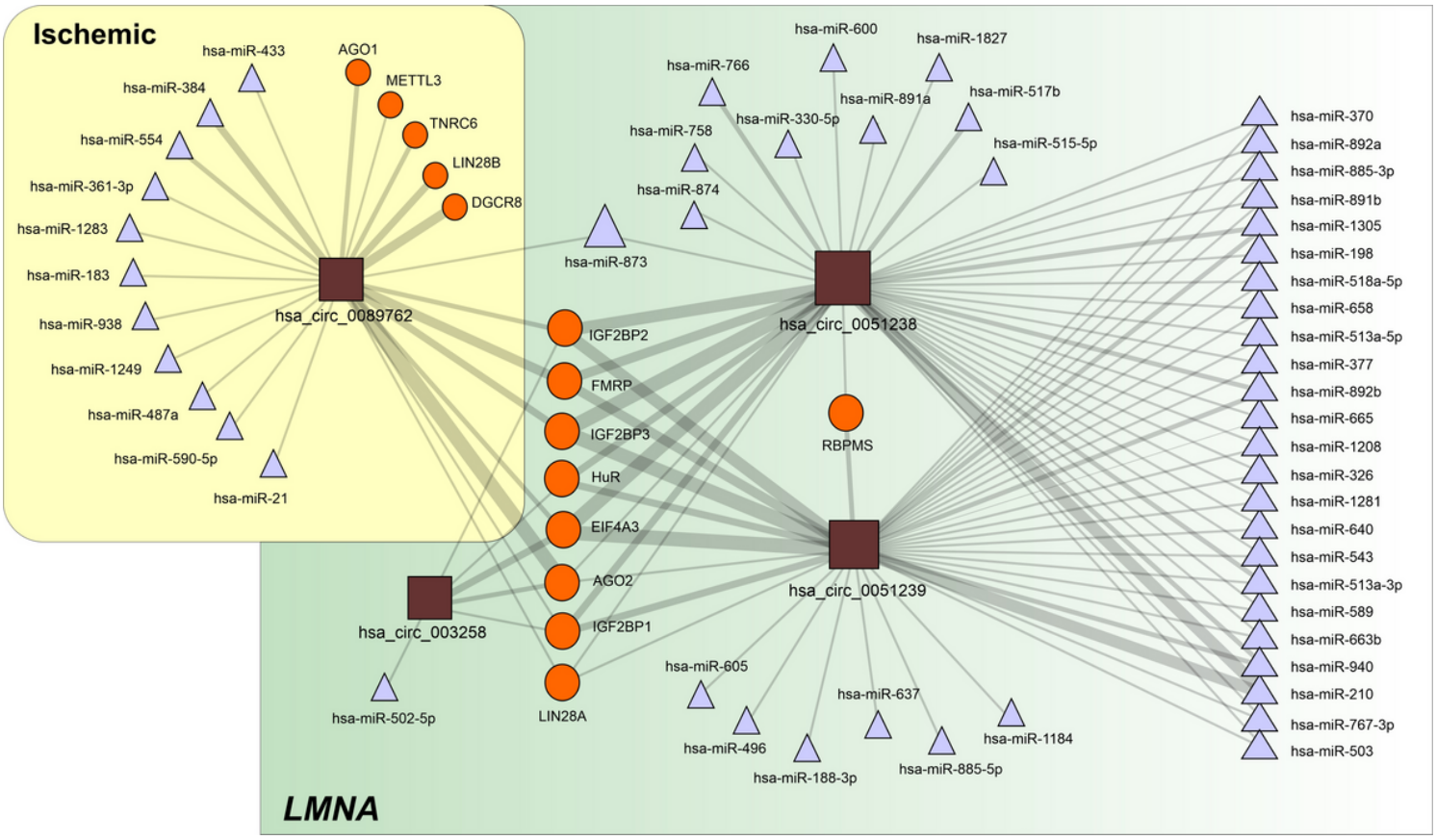

Figure 4

circRNA-centered regulatory network established among the selected circRNAs. The depicted interactions are based on data extracted from the circInteractome database and include miRNAs and RBPs. CircRNAs are represented as squares, RBPs as circles and miRNAs as triangles. The size of each symbol is proportional to the number of interactions established. The edge thickness is also proportional to the number of targets for each interacting partner as included in the circInteractome database. The regulatory network was prepared with Navigator software[14]. Abbreviations: DCM, dilated cardiomyopathy; LMNA, Lamin A/C gene; miRNA, microRNA; RBP, RNA binding protein.

Supplementary Files

This is a list of supplementary files associated with this preprint. Click to download.

- Supplementarymaterial.pdf